

Far-infrared spectroscopy in the spin-Peierls compound CuGeO_3 under high magnetic fields

K. Takehana, T. Takamasu, M. Hase, and G. Kido

Physical Properties Division, National Research Institute for Metals, 3-13 Sakura, Tsukuba-city, Ibaraki 305-0003, Japan

K. Uchinokura

Department of Advanced Materials Science, The University of Tokyo, 6th Engineering Building, 7-3-1 Hongo, Bunkyo-ku, Tokyo 113-8656, Japan

(Received 20 March 2000)

Polarized far-infrared (FIR) spectroscopic measurements and FIR magneto-optical studies were performed on the inorganic spin-Peierls compound CuGeO_3 . An absorption line, which was found at 98 cm^{-1} in the dimerized phase (D phase), was assigned to a folded phonon mode of B_{3u} symmetry. The splitting of the folded mode into two components in the incommensurate phase (IC phase) has been observed. A broad absorption centered at 63 cm^{-1} was observed only in the $\mathbf{E} \parallel b$ axis polarization, which was assigned to a magnetic excitation from singlet ground state to a continuum state.

I. INTRODUCTION

The discovery of the spin-Peierls (SP) transition in an inorganic compound CuGeO_3 (Ref. 1) has produced great interest in the properties of this quasi-one-dimensional $S = 1/2$ Heisenberg antiferromagnet. The lattice dimerization induced by the SP transition was confirmed by observation of superlattice Bragg peaks by electron diffraction,² x-ray and neutron diffraction.^{3,4} At low temperatures, a high magnetic field above 12 T induces a phase transition from the dimerized phase (D phase) to a magnetic phase.⁵ The high-field phase was assigned to an incommensurate phase (IC phase) based on the appearance of a splitting of the superlattice reflections above the critical field, H_C .⁶ Higher-order harmonics of the incommensurate Bragg reflections, which indicates that the lattice modulation forms a soliton lattice, were observed just above H_C by the x-ray experiments.⁷ An anomalous spontaneous strain appears with the SP transition and increases with decreasing temperature.⁸ This strain is partially removed at the transition from the D to the IC phase and continues to decrease with increasing field, as observed by magnetostriction measurements under high magnetic fields.^{9,10}

Since the coupling between the one-dimensional spin system and three-dimensional phonon fields plays an essential role in the SP transition, it is important to investigate the phonons related with the transition such as folded phonons and a soft phonon. The crystal structure of CuGeO_3 belongs to $Pbmm$ symmetry at room temperature.¹¹ According to the factor group analysis, optically active phonons are 12 modes [$4A_g(aa,bb,cc) + 4B_{1g}(ab) + 3B_{2g}(ac) + B_{3g}(bc)$] in the Raman spectra and 13 modes [$3B_{1u}(\mathbf{E} \parallel c) + 5B_{2u}(\mathbf{E} \parallel b) + 5B_{3u}(\mathbf{E} \parallel a)$] in the infrared spectra. All of them have already been assigned in the Raman and infrared spectra.¹² In the SP state, the symmetry is lowered to $Bbcm$ due to the formation of the superlattice^{4,13} and additional 18 Raman-active modes [$4A_g(aa,bb,cc) + 5B_{1g}(ab) + 4B_{2g}(ac) + 5B_{3g}(bc)$] and 9 infrared-active modes [$2B_{1u}(\mathbf{E} \parallel c) + 4B_{2u}(\mathbf{E} \parallel b) + 3B_{3u}(\mathbf{E} \parallel a)$] should appear below T_{SP} . At

present, three Raman modes at 107, 369, and 820 cm^{-1} were assigned to the A_g folded phonons in the D phase, while the first one has a Fano-type line shape.¹⁴⁻¹⁶ Concerning the infrared-active folded phonons, one B_{1u} and two B_{2u} modes were found at 284.2, 311.7, and 800 cm^{-1} , respectively.^{17,18} Besides those three infrared active modes, we assigned the absorption line at 98 cm^{-1} to a folded phonon in our previous paper, while its polarization properties were unclear.¹⁹

The field dependence of the folded phonon modes was investigated in the Raman experiments.^{20,21} The intensity decreases steeply at the boundary between the D and IC phases, while no energy shift was observed. Just above H_C , the intensity decreases to about half of the D phase, and continues to decrease in the IC phase with increasing field.²¹ In contrast to these results, however, the folded phonon mode at 98 cm^{-1} was unobservable in the IC phase in our previous paper.¹⁹

Magnetic excitations across the gap between the singlet ground state and the triplet excited state were found below T_{SP} in the far-infrared (FIR) measurements^{19,22-25} and continuous excitations between 30 and 230 cm^{-1} due to two magnon processes were observed below 60 K in the Raman experiments.^{14-16,26} Interestingly, two magnetic excitations were found at 19 cm^{-1} and 44 cm^{-1} by the electron spin resonance (ESR) measurements.^{22,25} Both modes split into two components in the presence of the magnetic field and become unobservable in the IC phase. In a recent inelastic neutron scattering (INS) experiment, Lorenzo *et al.* found a second magnetic excitation branch with a non-negligible spectral weight, which indicates that there are two magnetic excitation gaps of 19 cm^{-1} and 44 cm^{-1} at the zone center.²⁷ The authors concluded that its existence originates from the presence of the Dzyaloshinskii-Moriya (DM) anti-symmetric exchange terms, whose existence has also been suggested from ESR measurements.²⁸ In principle, magnetic excitations between the singlet and the triplet states are infrared inactive. Uhrig suggested that the observation of the gap at 44 cm^{-1} is caused by the presence of the staggered magnetic field in analogy to NENP [$\text{Ni}(\text{C}_{2\text{H}_8\text{N}_2)_2\text{NO}_2(\text{ClO}_4)$] and NINO [$\text{Ni}(\text{C}_{3\text{H}_{10}\text{N}_2)_2\text{NO}_2(\text{ClO}_4)$].²⁹ Their model does

not explain the observation in zero field and the field dependence of the intensity, so the microscopic mechanism of the magnetic excitation at 44 cm^{-1} is still unclear. Three new branches were found in the IC phase by the FIR experiments.²⁴ One of them originates from the discommensuration because of its appearance only just above H_C and others were explained as the absorption involving magnetic and vibrational excitations in a modulated structure. On the other hand, in the IC phase, suppression of the continuous structure between 30 and 230 cm^{-1} , especially the peak at 30 cm^{-1} ,²⁰ and enhancement of the peak at 17 cm^{-1} were observed in the Raman experiments.²¹

In order to clarify the property of the 98-cm^{-1} mode, we presented in this paper the polarized spectroscopic measurements on CuGeO_3 in zero field and magneto-optical studies up to 18 T .

II. EXPERIMENT

A CuGeO_3 single crystal was grown by a floating zone method using an image furnace and was cleaved along the (100) plane. We used a wedge-shaped sample with dimension of $1.5 \times 4 \times 6\text{ mm}^3$ in order to avoid the interference of FIR light in the sample.

FIR transmission was measured in the spectral range between 15 and 300 cm^{-1} with a minimum resolution of 0.1 cm^{-1} using a Fourier transform spectrometer (BOMEM DA8). The spectra were measured by using $50, 100\text{-}\mu\text{m}$ Mylar and Ge, Si coated $6\text{-}\mu\text{m}$ Mylar beamsplitters. An FIR polarizer of free-standing wire grid type with a grid period of $12.5\text{ }\mu\text{m}$ was used for polarized measurements. A Si bolometer that was operated at 4.2 K and a Si composite bolometer operated at 0.3 K were employed as the FIR detectors. The former was used for the higher-energy region than 50 cm^{-1} and the latter for the lower region. A high-pressure mercury lamp was used as a light source. The unpolarized spectra in the presence of magnetic field were obtained with an 18-T superconducting magnet in the Faraday configuration. Both the spectrometer and the detector were placed 3 m apart from the magnet in order to avoid the leakage flux of the magnet. The FIR light was led by an optical pipe system, which consisted of well-polished brass pipes (10 mm i.d.) and mirror cells that turn the FIR light direction through a right angle.³⁰ All the optical path is evacuated to avoid the absorption due to water vapor. The temperature dependence of the spectra was investigated down to 3 K .

III. RESULTS

A. $B=0\text{ T}$

Figures 1(a) and 1(b) show the transmission spectrum of CuGeO_3 in the $\mathbf{E}\parallel b$ and $\mathbf{E}\parallel c$ axis configuration, respectively, at $T=17\text{ K}$. Absorptions due to the optical phonons are clearly observed at 48 cm^{-1} and 135 cm^{-1} in Fig. 1(a) and at 135 and 170 cm^{-1} in Fig. 1(b), which were assigned to B_{2u} , B_{3u} , B_{3u} , and B_{1u} modes, respectively, by the infrared reflectivity measurements.¹² The appearance of B_{3u} modes in both the $\mathbf{E}\parallel b$ and $\mathbf{E}\parallel c$ configurations would be due to an inclination of a few degrees from the correct configuration.

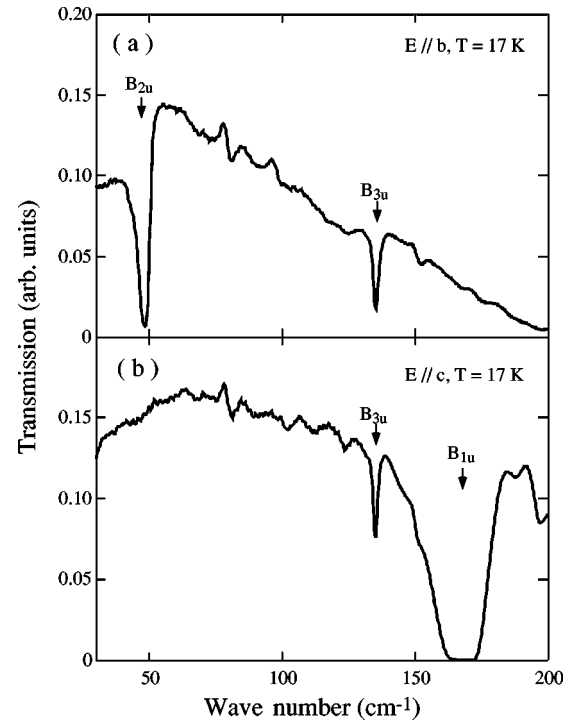


FIG. 1. Polarized transmission spectra at $B=0\text{ T}$ and $T=17\text{ K}$ in the (a) $\mathbf{E}\parallel b$ axis and (b) $\mathbf{E}\parallel c$ axis configurations.

In order to clarify the small change between the three phases; i.e., the uniform (U), D , and IC phase, the transmission spectra were normalized by the spectrum in the U phase, [$\text{Tr}(T=17\text{ K}, B=0\text{ T})$]. Figures 2(a) and 2(b) show the normalized spectra in the $\mathbf{E}\parallel b$ and $\mathbf{E}\parallel c$ configurations, respectively. A sharp absorption line at 98 cm^{-1} , which is labeled as FP in Fig. 2(a), appears only in the $\mathbf{E}\parallel b$ configuration below T_{SP} . The absorption intensity of FP decreases without broadening when the temperature increases up to T_{SP} and it shows no energy shift as a function of temperature. No structure was observed around 98 cm^{-1} in the 30-K spectrum, which indicates that FP appears only below T_{SP} . An asymmetric absorption, $M1$, which has a tail on the lower-energy side, was observed at 44 cm^{-1} only in the spectra of $\mathbf{E}\parallel b$ ($\mathbf{H}\parallel c$) configuration.¹⁷ $M1$ loses its intensity rapidly with broadening and its peak position shifts slightly toward lower energy when the temperature increases up to T_{SP} . The broad absorption, $M2$, which is centered at 63 cm^{-1} and has a wide tail on the higher-energy side, was newly found only in the $\mathbf{E}\parallel b$ ($\mathbf{H}\parallel c$) configuration below T_{SP} and grows with decreasing temperature, whose temperature dependence and polarization property are quite similar to that of $M1$. The structures around 50 cm^{-1} in the $\mathbf{E}\parallel b$ configuration, OP, are due to the temperature dependence of the B_{2u} optical phonon. On the other hand, no significant structure was observed in the spectra of $\mathbf{E}\parallel c$ configuration in both the U and the D phases.

In order to examine the polarization property of FP mode, an angular dependence was measured as shown in Fig. 3, when the sample is rotated around the b axis (see upper inset of Fig. 3), which means that the component of $\mathbf{E}\parallel a$ polarization becomes mixed into the spectrum when the angle θ increases from zero degrees. The absorption intensity increases almost linearly without energy shift and broadening,

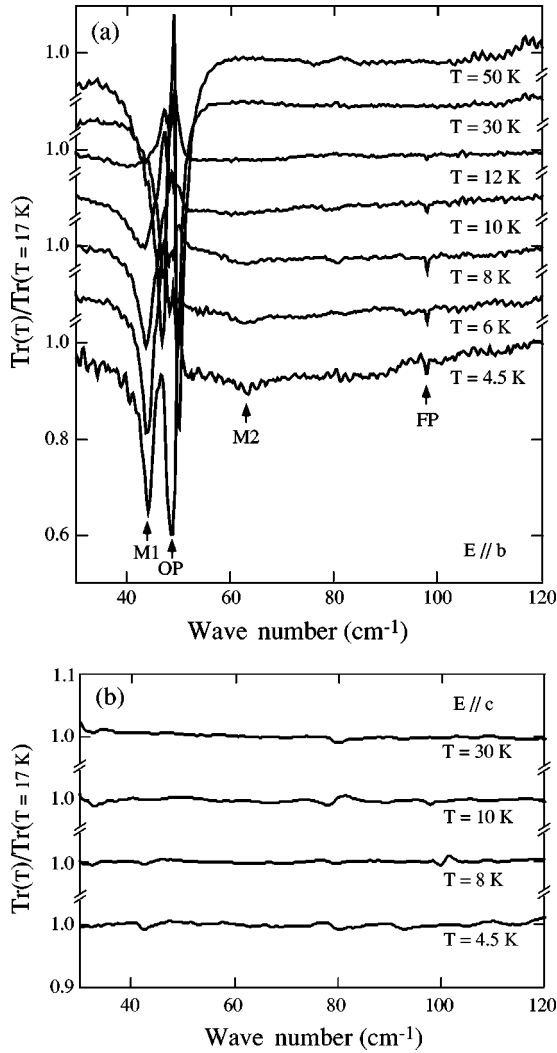


FIG. 2. (a) Normalized spectra, $\text{Tr}(T)/\text{Tr}(T=17\text{ K})$, in the configuration of the $\mathbf{E}\parallel b$ axis polarization at $B=0\text{ T}$. The absorptions at 44 cm^{-1} , 63 cm^{-1} , and 98 cm^{-1} below T_{SP} grow with decreasing temperature. The structures around 50 cm^{-1} , which appear in all spectra, are caused by temperature dependence of the B_{2u} optical phonon at 48 cm^{-1} . (b) Normalized spectra, $\text{Tr}(T)/\text{Tr}(T=17\text{ K})$, in the configuration of the $\mathbf{E}\parallel c$ axis polarization at $B=0\text{ T}$. No significant structure was observed.

as θ increases up to 40° (see lower inset of Fig. 3). According to these results, we conclude that the FP mode must have the $\mathbf{E}\parallel a$ polarization property. Observation of this mode in the $\mathbf{E}\parallel b$ configuration, as shown in Fig. 2(a), would be caused by the sample tilting by a few degrees from the correct configuration, because the modes of $\mathbf{E}\parallel a$ polarization must not be observed in the correct $\mathbf{E}\parallel b$ configuration. The absorption intensity at $\theta=30^\circ$ increases with decreasing temperature, as shown in the inset of Fig. 4. The temperature dependence of its intensity is well described by the power law $\alpha(T_{\text{SP}}-T)^{2\beta}$ (see Fig. 4). The best fit was obtained for $2\beta=0.55$, which is in good agreement with that of other folded phonons,^{17,18} the superlattice reflections,⁴ and the spontaneous strains.³¹ The intensity of folded phonons in zero field is proportional to the square of the lattice distortion induced by the SP transition, as well as that of superlattice reflections and the spontaneous strains.³¹

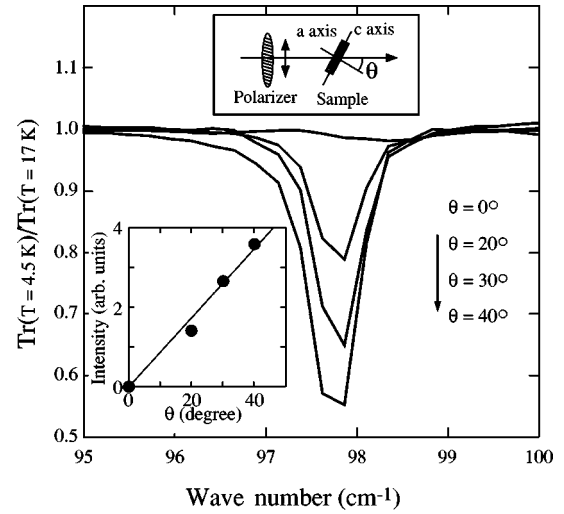


FIG. 3. Angular dependence of the absorption at 98 cm^{-1} for rotation of the sample around the b axis (see upper inset). As shown in the lower inset, the intensity increases almost linearly up to 40° .

B. $B \neq 0\text{ T}$

The normalized spectra in the presence of magnetic fields are shown in Fig. 5. The FP mode was observed in this configuration, which may be caused by an inclination of the sample, as mentioned above. Both peak position and peak intensity remain unchanged up to H_C and become unclear above H_C . In the presence of a magnetic field, $M1$ splits into two components, $M1_U$ and $M1_L$, which correspond to the excitations from the singlet ground state to the $m_S = \pm 1$ branches of the triplet excited states. From the field dependence of the peak positions, we estimate the g value as $g=2.1$, which is in good agreement with the reported values.^{22,24} Neither $M1_U$ nor $M1_L$ are observed in the IC phase, which is again in agreement with the previous results.²²⁻²⁵ With increase of magnetic field $M2$ shifts toward higher energy, while it could not be confirmed whether the lower branch exists or not, owing to overlap with $M1_U$

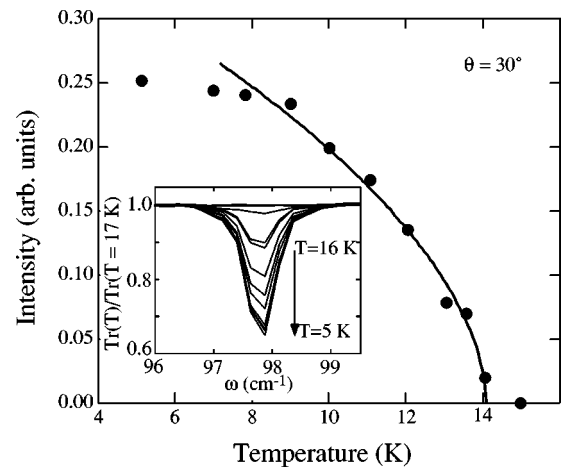


FIG. 4. Temperature dependence of the intensity of the absorption at 98 cm^{-1} , when the sample is rotated by 30° around the b axis, which is well described by the power law, $\alpha(T_{\text{SP}}-T)^{2\beta}$. The inset shows that the absorption at 98 cm^{-1} increases with decreasing temperature.

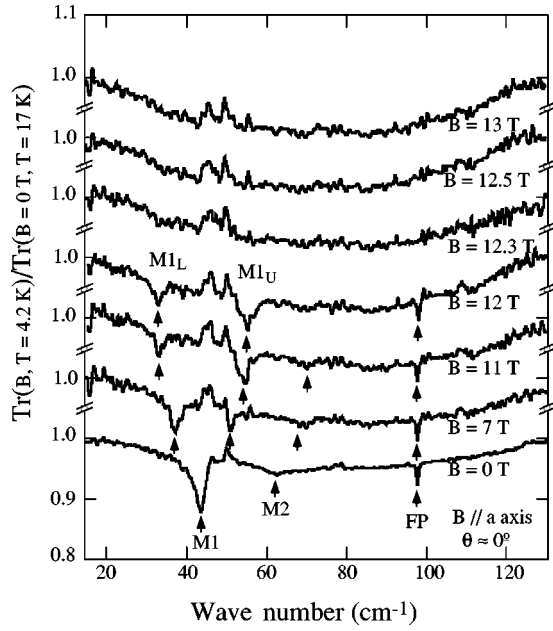


FIG. 5. Unpolarized normalized spectra, $\text{Tr}(B, T = 4.2 \text{ K})/\text{Tr}(B = 0 \text{ T}, T = 17 \text{ K})$, for various fields, when the sample was tilted by a few degrees from the $\mathbf{B} \parallel a$ axis configuration.

branch. Around and above H_C , $M2$ becomes broader. There is no significant change of $M2$ at H_C .

In order to clarify the behavior of FP mode in the IC phase, the field dependence of the spectrum was investigated up to 18 T with the sample inclined around the b axis by about 20° (see Fig. 6). We have observed that two absorption

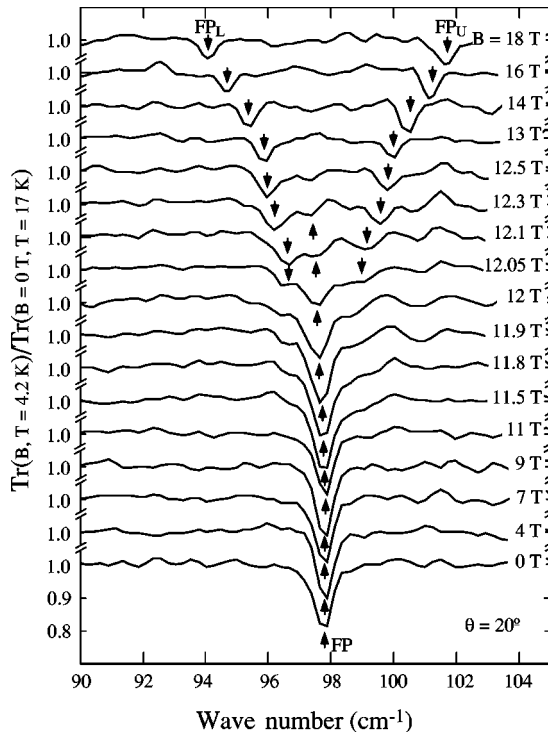


FIG. 6. Field dependence of the absorption at 98 cm^{-1} at 4.2 K, when the sample is rotated by 20° . Satellite peaks appear on both sides of the absorption at 98 cm^{-1} in the IC phase, while the main peak weakens and disappears around H_C .

TABLE I. Folded phonon modes that appear in the FIR spectra below T_{SP} . The first one is the mode found in this study.

Frequency ω (cm^{-1})	Polarization	IC phase (above H_C)
98	$\mathbf{E} \parallel a$	splitting
284.2 ^a	$\mathbf{E} \parallel c$	
311.7 ^b	$\mathbf{E} \parallel b$	detectable ^c
800 ^d	$\mathbf{E} \parallel b$	

^aFrom Ref. 18.

^bFrom Ref. 18.

^cFrom Ref. 32.

^dFrom Ref. 17.

lines, FP_U and FP_L , appear on both sides of FP with approximately the same intervals around H_C , while FP loses its intensity with slightly shifting to lower energy and vanishes above 12.3 T. The energy separation between FP_U and FP_L , $\Delta\omega$, increases with increasing field.

IV. DISCUSSION

Table I shows the folded phonons that have been found by the FIR studies up to now. Four folded phonons have been found among the nine modes predicted by the factor group analysis. The reason why the remaining modes are not observed might be due to their weak intensity or concealment in other strong optical phonons. The folded mode of 311.7 cm^{-1} was observed above H_C , but the details were unclear because it is located on the shoulder of an optical phonon.³² The field dependence of the folded modes of 284.2 and 800 cm^{-1} have not been reported yet.

The peak positions of FP, FP_U , and FP_L at $\theta = 20^\circ$ are shown in the Fig. 7 as functions of magnetic field. The absorptions, FP_U and FP_L , were confirmed in the spectrum of the IC phase in Fig. 5, although their intensity is quite small. The peak positions at $\theta \approx 0^\circ$, which are also plotted in Fig. 7,

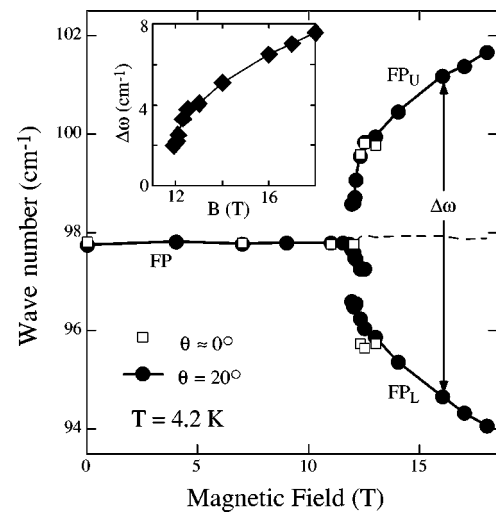


FIG. 7. Field dependence of the peak positions of the absorption at 98 cm^{-1} and its satellites at 4.2 K, when the sample is rotated by a few degrees (open squares) and 20° (closed circles). The dashed line indicates the field dependence of the average energy of the satellites. Inset shows the field dependence of the energy separation between these satellites, $\Delta\omega$.

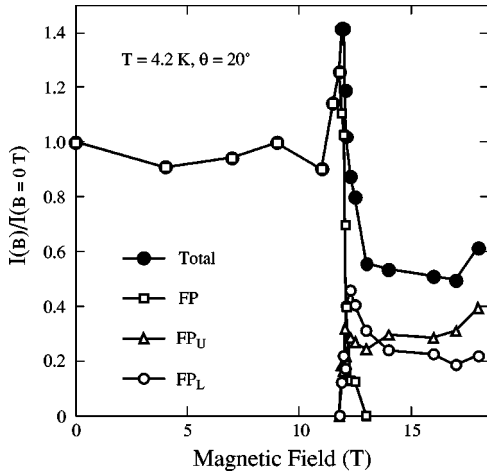


FIG. 8. Field dependence of the integrated intensities of the absorption at 98 cm^{-1} , its satellites, FP, FP_L , FP_U and their total at 4.2 K, normalized to zero field.

are in good agreement with the result at $\theta=20^\circ$, where deviations of H_C caused by the inclination are quite small. This agreement indicates that appearance of FP_U and FP_L instead of FP in the IC phase is not caused by the sample inclination, but is an intrinsic property of this mode. FP is observed in the D phase and both FP_U and FP_L are observed in the IC phase. They coexist in the vicinity of the boundary between the D and IC phases, which is quite similar to the behavior of the superlattice reflection in the x-ray measurements.⁶ The energy of FP is independent of the static magnetic field and the temperature in the D phase. It slightly shifts toward lower energy in the coexistence region, which may be caused by a strong decrease of the spontaneous strain when going from the D to IC phase,¹⁰ or by discommensurations which appear in the vicinity of the phase boundary. The positions of FP_U and FP_L are almost symmetrical with respect to that of FP, which indicates that FP line splits into two lines; FP_U and FP_L , in the IC phase. $\Delta\omega$ increases steeply with increasing field at the vicinity of the phase boundary and the rate of the increase slows down gradually with increasing field (see inset of Fig. 7). The field dependence of the integrated intensities of FP, FP_U , and FP_L and their total are displayed in Fig. 8. The intensity of FP decreases steeply to zero just above H_C after enhancement at the vicinity of the phase boundary, while it is almost field independent below 10 T. Similar enhancements around H_C were observed in the field dependence of both FP_U and FP_L . Total intensity in the IC phase decreases to about 50% of zero-field value and gradually decreases with increasing field. This behavior is quite similar to that of other folded phonons except for the enhancement around H_C .^{20,21} The enhancement was also observed in the Fano-type mode at 107 cm^{-1} , but was much more moderate.²¹ The intensity of folded phonons is closely related to the lattice distortion induced by the SP transition, as well as to the intensity of the superlattice reflections. For this reason, the field dependence of the intensity of the folded phonon,²¹ the superlattice reflection,⁶ and the spontaneous strain¹⁰ quite resemble each other. However, enhancements around H_C were only observed in this mode and a Fano-type folded mode in the Raman experiments, which would suggest the presence of some interaction which causes

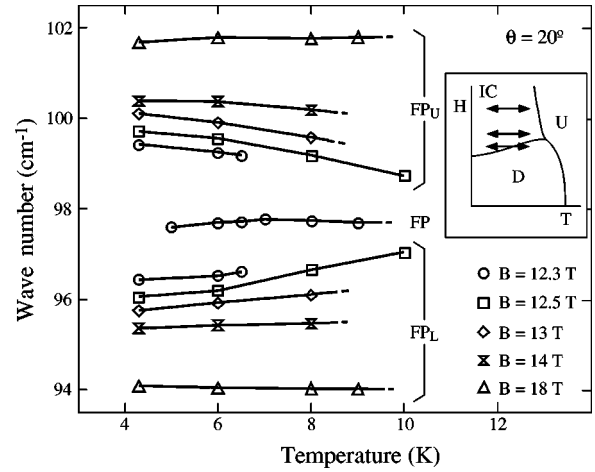


FIG. 9. Temperature dependence of the peak positions of FP, FP_U , and FP_L at various fixed fields. The inset shows the schematic phase diagram in the (H, T) plane.

the splitting of this mode in the IC phase.

The temperature dependence of the peak positions of FP, FP_U , and FP_L in various fixed fields is shown in Fig. 9. The symmetrical location of FP_U and FP_L with respect to FP is also confirmed in Fig. 9. The intensity decreases steeply with approaching the D - U phase or the IC- U phase boundary, and these peaks disappear in the U phase. FP_U and FP_L shift toward lower and higher energy, respectively, which means that $\Delta\omega$ decreases with increasing temperature. The temperature dependence of the peak positions becomes weak with increasing field, and the peak positions at 18 T are almost independent of temperature. A possible explanation for this temperature dependence is as follows: $\Delta\omega$ decreases with approaching the D -IC phase boundary, corresponding to the field dependence of $\Delta\omega$ as shown in Fig. 7. When the magnetic field is just above H_C , the magnetic state approaches the phase boundary with increasing temperature and this tendency gets weaker for $H \gg H_C$, according to the shape of the phase boundary (see the inset of Fig. 9).

To our knowledge, this is the first example of the observation of splitting of the folded phonon in the IC phase. The field dependence of $\Delta\omega$ quite resembles that of the incommensurability, ΔL , which was estimated by the splitting of the (3.5, 1, 2.5) superlattice reflection in the x-ray diffraction experiments.⁷ The temperature dependence of $\Delta\omega$ is also consistent with that of ΔL , while the latter was investigated only just above H_C .⁶ We compared the field dependence of $\Delta\omega$ and ΔL by scaling them with H_C , as shown in Fig. 10. Critical behavior of ΔL in pure and diluted CuGeO_3 can be scaled by a universal curve, although there are some deviations dependent on the composition. The universal curve is well described by the function $1/\ln[8H_C/(H-H_C)]$, which is predicted by the mean-field theory.³³ The right scale was adjusted to fit $\Delta\omega$ to the universal curve. It is obvious that $\Delta\omega$ is also well described by the same universal curve. Moreover, $\Delta\omega$ approaches gradually the theoretically predicted curve in the high magnetic field limit by Cross.³⁴ These results suggest that $\Delta\omega$ is proportional to the incommensurability, at least up to 18 T.

In principle, optical excitations are allowed to be infrared active only at $\mathbf{k}=\mathbf{0}$ owing to the momentum conservation

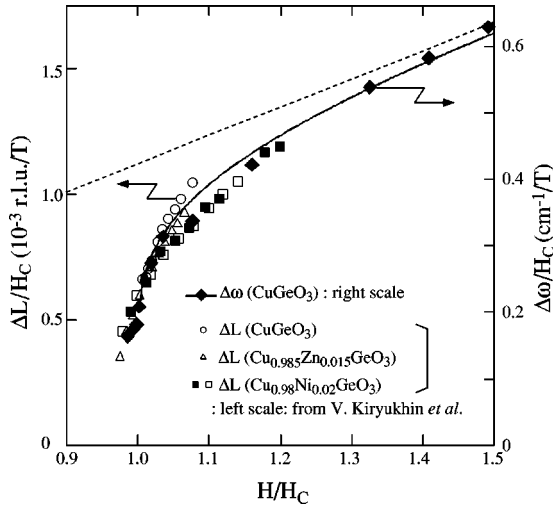


FIG. 10. Field dependence of the energy separation between PF_L and FP_U , $\Delta\omega$, and that of the incommensurability, ΔL , which were measured by Kiryukhin *et al.* (Ref. 7). Both $\Delta\omega$ and ΔL are scaled by the respective critical field, H_C , and can be well described by the theoretical curve $1/\ln[8H_C/(H-H_C)]$ within the mean field theory (Ref. 33). The dashed line indicates the theoretical prediction by Cross for the high magnetic field limit (Ref. 34).

rule. When the lattice modulation is induced, excitations at $\mathbf{k} = \pm n\mathbf{q}$ are allowed in addition to those at $\mathbf{k} = 0$, where \mathbf{q} is the modulation wave vector and n is an integer, although the intensities decrease rapidly with increasing n .³⁵ In the case of the SP transition, $\mathbf{q} = \mathbf{q}_{SP}$, where \mathbf{q}_{SP} is the modulation wave vector caused by the SP phase transition, which is located on the zone boundary in the U phase. This means that the excitations at the zone boundary in the U phase are folded to the zone center. This makes the folded phonons observable below T_{SP} . In the IC phase, \mathbf{q} deviates from \mathbf{q}_{SP} by a certain wave number $\Delta\mathbf{q}$, which makes the excitations at $\mathbf{k} = \pm(\mathbf{q}_{SP} - \Delta\mathbf{q})$ infrared active. These modes have the same wavelength as the incommensurability and propagate along the c axis toward the opposite direction from each other. Experimentally, the average component of the spin polarization was confirmed to have a periodicity of $2\Delta\mathbf{q}$ by the NMR (Ref. 36) and the neutron scattering studies,³⁷ while the staggered component has a periodicity of $\pm(\mathbf{q}_{SP} - \Delta\mathbf{q})$. Note that $2\Delta\mathbf{q}$ is equivalent with the difference between $\pm(\mathbf{q}_{SP} - \Delta\mathbf{q})$. When the two modes of $\mathbf{k} = \pm(\mathbf{q}_{SP} - \Delta\mathbf{q})$ have the strong spin-phonon coupling, mixing of these modes and the splitting of the mixed modes are caused by the interaction between these two modes through the modulation of the spin polarization with the periodicity of $2\Delta\mathbf{q}$. Therefore, if we define κ as the coupling between the $\pm(\mathbf{q}_{SP} - \Delta\mathbf{q})$ modes, κ is certainly nonzero. The energy separation can be described as follows:

$$\begin{vmatrix} \omega_0^2 - \omega^2 & \kappa \\ \kappa^* & \omega_0^2 - \omega^2 \end{vmatrix} = 0, \quad (4.1)$$

$$\omega^2 = \omega_0^2 \pm |\kappa|, \quad (4.2)$$

$$\omega \approx \omega_0 \pm \frac{|\kappa|}{2\omega_0}, \quad (4.3)$$

where ω is the absorption energy with the coupling, ω_0 is that without the coupling. Equation (4.3) means that the absorption is split into two components and they appear on both sides of ω_0 with the same separations, which is quite consistent with the experimental results. It also suggests that $\Delta\omega$ is proportional to $|\kappa|$. The eigenstates with the energy $\omega_0 \pm |\kappa|/2\omega_0$ are two kinds of the standing waves having the same period as the incommensurability and different phases. $|\kappa|$ is dependent on both temperature and magnetic field, because the incommensurability is strongly dependent on them. The field dependence of $\Delta\omega$ is in good agreement with that of the magnetization.³⁶ The temperature dependence of $\Delta\omega$ is also consistent with that of the magnetization.³⁸ It would be a reasonable assumption that $|\kappa|$ is proportional to the magnetization, i.e., the density of the solitons, because we argued that the coupling to the average component of the spin polarization causes the energy splitting. Therefore, $|\kappa|$ is proportional to Δq , which leads to the relation that $\Delta\omega$ is proportional to Δq . This conclusion is quite consistent with our experimental results. Note that there is no other example than FP to have the splitting of the folded mode in the IC phase, while the above argument may be applied also to any other modes. This indicates that FP is the particular mode to have the strong coupling to the average component of the spin polarization. In general, the spin-Peierls system has the spin-phonon coupled modes, and one of them is the soft mode that softens toward T_{SP} .³⁴ The soft phonon mode has not been found yet, and is now believed to be nonexistent in CuGeO_3 . Since CuGeO_3 is a spin-Peierls system, there should be the spin-phonon coupled modes, even though none of them exhibits softening. Braden *et al.* argued the possibility of the spin-phonon coupling of the phonon modes at the zone boundary that become the Raman-active modes in the D phase, and observed the anomalous hardening of these two modes with lower frequencies above T_{SP} in the INS experiments, while no soft mode behavior was observed around T_{SP} .³⁹ The anomalous hardening was explained as the pretransitional fluctuations of the Peierls-active phonon modes, by reconsidering Cross and Fischer's approach.⁴⁰ The energy of the FP mode is the lowest among those of the folded phonon modes that have been found up to now, and is just close to that of the lowest folded mode with Raman activity, which was argued to have the strong spin-phonon coupling. The splitting in the IC phase is considered as the proof that FP has the strong spin-phonon coupling. It also indicates the possibility of FP to be one of the phonon modes contributing to the mechanism of the spin-Peierls transition, similar to the Raman active modes as was argued in Ref. 39. The intensities of both the split-off branches of the superlattice reflection in the IC phase would be a quarter of that in the D phase, on the assumption that the lattice modulation in the IC phase is described as the sinusoidal wave $\delta \cos(\Delta\mathbf{q} \cdot \mathbf{r})$, where δ is the magnitude of the lattice modulation in the D phase. This was confirmed in the experimental results.⁶ Similarly, the intensities of the folded phonon modes at $\mathbf{k} = \pm(\mathbf{q}_{SP} - \Delta\mathbf{q})$ in the IC phase would be a quarter of that at $\mathbf{k} = \mathbf{q}_{SP}$ in the D phase; that is, the total intensity in the IC phase is half that in the D phase. This is roughly in agreement with the results of this study. The intensities of other folded modes just above H_C also decrease to about half of that in the D phase.²¹ The enhancement of the intensity

TABLE II. Magnetic absorptions that appear in the FIR spectra below T_{SP} . The last one is the absorption band found in this study.

Frequency ω (cm^{-1}) (at 4.2 K)	Polarization (at 0 T)	D phase (below H_C)	IC phase (above H_C)
19 ^a		splitting	
44 ^b	$\mathbf{E}\parallel b > \mathbf{E}\parallel c$	splitting	
63	$\mathbf{E}\parallel b > \mathbf{E}\parallel c$	shifting	broadening

^aFrom Ref. 25.

^bFrom Ref. 22.

around H_C might be caused by the critical fluctuation of the spin system, because no anomaly was observed in the x-ray measurements.

Next we will discuss the broad absorption band $M2$. Table II shows the magnetic excitations which have been found by the FIR experiments. The absorption of 19 cm^{-1} has been observed only by using the FIR laser.²⁵ To our knowledge, $M2$ was found for the first time in this study, and the shift under the magnetic field indicates that $M2$ has a magnetic origin. Absorptions of both 19 and 44 cm^{-1} were assigned to the magnetic excitation from the singlet ground state to the triplet states, which means that there are two magnetic gaps at the Γ point. A second magnetic excitation branch, whose energy gap corresponds to 44 cm^{-1} at the Γ point, was found by the INS experiments.²⁷ The newly observed branch was assigned to the zone-folded one due to the existence of the DM antisymmetric exchange terms, which means that the energy gap of the new branch at the Γ point corresponds to that of the original branch at the zone boundary. The energy scan spectrum for the zone boundary $\mathbf{Q}=(0,2,0.5)$ was investigated by the INS experiments (see Fig. 2 of Ref. 41), and a continuum of magnetic excitations, whose peak is located at 7 meV , was found to be separated from the triplet branch by the second gap of 2 meV . We infer that $M2$ originates in a magnetic excitation at the Γ point from the singlet ground state to the continuum state spreading over the higher-energy region above the newly observed triplet branch. Note that not only the energy of $M1$, but also that of $M2$ coincide with those of the first and second peaks

at 5 meV and 7 meV , respectively, on the data for $\mathbf{Q}=(0,2,0.5)$ in the INS experiments (see Fig. 2 of Ref. 41). The line shapes of $M1$ and $M2$ also resemble those of the corresponding ones in the INS experiments. There are other similar features such as the ratio of two peaks and the long tail on the higher-energy side of the continuum of magnetic excitations. An ‘‘absorption valley’’ between $M1$ and $M2$ corresponds to the ‘‘second gap’’ found by the INS measurements. A possibility of an optical excitation between the singlet ground state and the continuum state was suggested by Kokado and Suzuki.⁴² The magnetic excitation at 19 cm^{-1} was found to be too weak to be observed in our experiments. Missing of the absorption at 19 cm^{-1} in this study would be connected to the small density of state of the magnetic excitation branches. The numerical studies without the DM interaction predicted that the density of states at the zone center is much smaller than at the zone boundary.⁴³ The ‘‘rampart’’ structure of the continuum state, which was found in the INS experiments around 30 meV ,⁴⁴ is expected to be observed, but has not been confirmed in our spectrum probably because of the strong absorption of other origins, as shown in Fig. 1. We have not only observed the magnetic excitation from the singlet state to the continuum state by the optical method, but also confirmed the presence of the second gap located at $5\text{--}7 \text{ meV}$ at the Γ point, which, to our knowledge, has not yet been observed in the INS experiments.

V. CONCLUSIONS

We have performed the polarized FIR spectroscopic measurements and the unpolarized FIR magneto-optical studies on the spin-Peierls compound CuGeO_3 . A sharp absorption line, which appears at 98 cm^{-1} in the D phase, was assigned to a folded phonon mode of B_{3u} symmetry. This folded mode was found to split into two components in the IC phase. The energy separation of the two split branches is proportional to the incommensurability in the IC phase. A broad absorption centered at 63 cm^{-1} was found in the $\mathbf{E}\parallel b$ axis polarization spectra, which was assigned to magnetic excitation from singlet ground state to a continuum state.

¹M. Hase, I. Terasaki, and K. Uchinokura, Phys. Rev. Lett. **70**, 3651 (1993).

²O. Kamimura, M. Terauchi, M. Tanaka, O. Fujita, and J. Akimitsu, J. Phys. Soc. Jpn. **63**, 2467 (1994).

³J. P. Pouget, L. P. Regnault, M. Ain, B. Hennion, J. P. Renard, P. Veillet, G. Dhalenne, and A. Revcolevschi, Phys. Rev. Lett. **72**, 4037 (1994).

⁴K. Hirota, D. E. Cox, J. E. Lorenzo, G. Shirane, J. M. Tranquada, M. Hase, K. Uchinokura, H. Kojima, Y. Shibuya, and I. Tanaka, Phys. Rev. Lett. **73**, 736 (1994).

⁵M. Hase, I. Terasaki, K. Uchinokura, M. Tokunaga, N. Miura, and H. Obara, Phys. Rev. B **48**, 9616 (1993).

⁶V. Kiryukhin and B. Keimer, Phys. Rev. B **52**, R704 (1995).

⁷V. Kiryukhin, B. Keimer, J. P. Hill, and A. Vigliante, Phys. Rev. Lett. **76**, 4608 (1996).

⁸J. E. Lorenzo, K. Hirota, G. Shirane, J. M. Tranquada, M. Hase,

K. Uchinokura, H. Kojima, I. Tanaka, and Y. Shibuya, Phys. Rev. B **50**, 1278 (1994).

⁹K. Takehana, M. Oshikiri, G. Kido, M. Hase, and K. Uchinokura, J. Phys. Soc. Jpn. **65**, 2783 (1996).

¹⁰K. Takehana, T. Takamasu, M. Hase, G. Kido, and K. Uchinokura, Physica B **246-247**, 246 (1998).

¹¹H. Völlenkle, A. Wittmann, and H. Nowotny, Monatsch. Chem. **98**, 1352 (1967).

¹²Z. V. Popović, S. D. Dević, V. N. Popov, G. Dhalenne, and A. Revcolevschi, Phys. Rev. B **52**, 4185 (1995).

¹³M. Braden, G. Wilkendorf, J. Lorenzana, M. Ain, G. J. McIntyre, M. Behruzi, G. Heger, G. Dhalenne, and A. Revcolevschi, Phys. Rev. B **54**, 1105 (1996).

¹⁴N. Ogita, T. Minami, Y. Tanimoto, O. Fujita, J. Akimitsu, P. Lemmens, G. Güntherodt, and M. Udagawa, J. Phys. Soc. Jpn. **65**, 3754 (1996).

- ¹⁵I. Loa, S. Gronemeyer, C. Thomsen, and R. K. Kremer, *Solid State Commun.* **99**, 231 (1996).
- ¹⁶P. H. M. van Loosdrecht, J. P. Boucher, G. Martinez, G. Dhalenne, and A. Revcolevschi, *Phys. Rev. Lett.* **76**, 311 (1996).
- ¹⁷A. Damascelli, D. van der Marel, F. Parmigiani, G. Dhalenne, and A. Revcolevschi, *Phys. Rev. B* **56**, R11 373 (1997).
- ¹⁸M. N. Popova, A. B. Sushkov, S. A. Golubchik, A. N. Vasil'ev, and L. I. Leonyuk, *Phys. Rev. B* **57**, 5040 (1998).
- ¹⁹K. Takehana, M. Oshikiri, T. Takamasu, M. Hase, G. Kido, and K. Uchinokura, *J. Magn. Magn. Mater.* **177-181**, 699 (1998).
- ²⁰P. H. M. van Loosdrecht, J. P. Boucher, G. Martinez, G. Dhalenne, and A. Revcolevschi, *J. Appl. Phys.* **79**, 5395 (1996).
- ²¹I. Loa, S. Gronemeyer, C. Thomsen, and R. K. Kremer, *Z. Phys. Chem. (Munich)* **201**, 333 (1997).
- ²²T. M. Brill, J. P. Boucher, J. Voiron, G. Dhalenne, A. Revcolevschi, and J. P. Renard, *Phys. Rev. Lett.* **73**, 1545 (1994).
- ²³G. Li, J. L. Musfeldt, Y. J. Wang, S. Jandl, M. Poirier, A. Revcolevschi, and G. Dhalenne, *Phys. Rev. B* **54**, R15 633 (1996).
- ²⁴P. H. M. van Loosdrecht, S. Huant, G. Martinez, G. Dhalenne, and A. Revcolevschi, *Phys. Rev. B* **54**, R3730 (1996).
- ²⁵H. Nojiri, H. Ohta, N. Miura, and M. Motokawa, *Physica B* **246-247**, 16 (1998).
- ²⁶H. Kuroe, T. Sekine, M. Hase, Y. Sasago, K. Uchinokura, H. Kojima, I. Tanaka, and Y. Shibuya, *Phys. Rev. B* **50**, 16 468 (1994).
- ²⁷J. E. Lorenzo, L. P. Regnault, J. P. Boucher, B. Hennion, G. Dhalenne, and A. Revcolevschi, *Europhys. Lett.* **45**, 619 (1999).
- ²⁸I. Yamada, M. Nishi, and J. Akimitsu, *J. Phys.: Condens. Matter* **8**, 2625 (1996).
- ²⁹G. S. Uhrig, *Phys. Rev. Lett.* **79**, 163 (1997).
- ³⁰K. Takehana, M. Oshikiri, G. Kido, A. Takazawa, M. Sato, K. Nagasaka, M. Hase, and K. Uchinokura, *Physica B* **216**, 354 (1996).
- ³¹Q. J. Harris, Q. Feng, R. J. Birgeneau, K. Hirota, K. Kakurai, J. E. Lorenzo, G. Shirane, M. Hase, K. Uchinokura, H. Kojima, I. Tanaka, and Y. Shibuya, *Phys. Rev. B* **50**, 12 606 (1994).
- ³²J. L. Musfeldt, Y. J. Wang, S. Jandl, M. Poirier, A. Revcolevschi, and G. Dhalenne, *Phys. Rev. B* **54**, 469 (1996).
- ³³A. I. Buzdin, M. L. Kubic, and V. V. Tugushev, *Solid State Commun.* **48**, 483 (1983).
- ³⁴M. C. Cross, *Phys. Rev. B* **20**, 4606 (1979).
- ³⁵T. Janssen, *J. Phys. C* **12**, 5391 (1979).
- ³⁶M. Horvatić, Y. Fagot-Revurat, C. Berthier, G. Dhalenne, and A. Revcolevschi, *Phys. Rev. Lett.* **83**, 420 (1999).
- ³⁷H. M. Rønnow, M. Enderle, D. F. McMorrow, L.-P. Regnault, G. Dhalenne, A. Revcolevschi, A. Hoser, K. Prokes, P. Vorderwisch, and H. Schneider, *Phys. Rev. Lett.* **84**, 4469 (2000).
- ³⁸H. Hori, M. Furusawa, T. Takeuchi, S. Sugai, K. Kindo, and A. Yamagishi, *J. Phys. Soc. Jpn.* **63**, 18 (1994).
- ³⁹M. Braden, B. Hennion, W. Reichardt, G. Dhalenne, and A. Revcolevschi, *Phys. Rev. Lett.* **80**, 3634 (1998).
- ⁴⁰C. Gros and R. Werner, *Phys. Rev. B* **58**, R14 677 (1998).
- ⁴¹M. Aïn, J. E. Lorenzo, L. P. Regnault, G. Dhalenne, A. Revcolevschi, B. Hennion, and Th. Jolicœur, *Phys. Rev. Lett.* **78**, 1560 (1997).
- ⁴²S. Kokado and N. Suzuki, in *Proceedings of the 4th International Symposium on Advanced Physical Fields*, Tsukuba, Japan, 1999, edited by G. Kido (unpublished).
- ⁴³S. Haas and E. Dagotto, *Phys. Rev. B* **52**, R14 396 (1995).
- ⁴⁴M. Arai, M. Fujita, M. Motokawa, J. Akimitsu, and S. M. Bennington, *Phys. Rev. Lett.* **77**, 3649 (1996).